Toll-Like Receptor 9 Signaling Regulates Tissue Factor and Tissue Factor Pathway Inhibitor Expression in Human Endothelial Cells and Coagulation in Mice

Driss El Kebir, PhD[1]; Anas Damlaj, MSc[1]; Nesrine Makhezer, MSc[1]; János G. Filep, MD[1,2]

Objective: Bacterial DNA (CpG DNA) persists in tissues and blood under pathological conditions that are associated with enhanced intravascular coagulation. Toll-like receptor 9 recognizes CpG DNA and elicits innate and adoptive immunity, yet the impact of CpG DNA on coagulation has not been studied. In this study, we investigated the effects of CpG DNA on the expression and activity of tissue factor, a key initiator of coagulation and tissue factor pathway inhibitor in human coronary artery endothelial cells and on coagulation in mice.
Design: Controlled in vitro and in vivo studies.
Setting: University research laboratory.
Subjects: Cultured human coronary artery endothelial cell, wild-type mice, and *TLR9*-deficient mice.
Interventions: Human coronary artery endothelial cell was challenged with CpG DNA, and tissue factor and tissue factor pathway inhibitor expression and activity were assessed. In mice, the effects of CpG DNA on bleeding time and plasma levels of thrombin-antithrombin complexes and tissue factor were measured.
Measurements and Main Results: We found that CpG DNA, but not eukaryotic DNA, evoked marked nuclear factor-κB-mediated increases in tissue factor expression at both messenger RNA and protein levels, as well as in tissue factor activity. Conversely, CpG DNA significantly reduced tissue factor pathway inhibitor transcription, secretion, and activity. Inhibition of Toll-like receptor 9 with a telomere-derived Toll-like receptor 9 inhibitory oligonucleotide or transient Toll-like receptor 9 knockdown with small interfering RNA attenuated human coronary artery endothelial cell responses to CpG DNA. In wild-type mice, CpG DNA shortened the bleeding time parallel with dramatic increases in plasma thrombin-antithrombin complex and tissue factor levels. Pretreatment with inhibitory oligonucleotide or anti-tissue factor antibody or genetic deletion of *TLR9* prevented these changes, whereas depleting monocytes with clodronate resulted in a modest partial inhibition.
Conclusions: Our findings demonstrate that bacterial DNA through Toll-like receptor 9 shifted the balance of tissue factor and tissue factor pathway inhibitor toward procoagulant phenotype in human coronary artery endothelial cells and activated blood coagulation in mice. Our study identifies Toll-like receptor 9 inhibitory oligonucleotides as potential therapeutic agents for the prevention of coagulation in pathologies where bacterial DNA may abundantly be present. (*Crit Care Med* 2015; 43:e179–e189)
Key Words: bacterial DNA; coagulation; endothelial cell; nuclear factor-κB; tissue factor; Toll-like receptor 9

Innate immunity is triggered by receptors that sense pathogen-associated molecular patterns. Bacterial DNA, containing unmethylated CpG dinucleotide motifs (CpG DNA), and mitochondrial DNA are potent inducers of immune responses during infection and tissue damage (1–4). CpG DNA released from proliferating bacteria or following killing of bacteria may persist in tissues or blood even in the absence of bacteria and contribute to ongoing inflammation. CpG DNA has been detected in atherosclerotic plaques in human coronary arteries (5) and in the blood of critically ill patients who have had negative blood culture for bacteria (6). To date, Toll-like receptor (TLR) 9 remains the only known receptor for immunostimulatory DNA (7, 8). TLR9 was first identified in antigen presenting cells (7) consistent with the role of these cells in immune surveillance. TLR9 is also expressed in nonimmune cells, including

human umbilical vein endothelial cells (HUVECs) (9), dermal microvascular (10) and lymphatic endothelial cells (11), and endothelial cells of human atherosclerotic plaques (12). CpG DNA was found to stimulate expression of adhesion molecules, interleukin (IL)-8, and monocyte chemoattractant protein-1 in HUVECs (9), whereas it suppressed IL-8 release from microvascular endothelial cells (10). The impact of CpG DNA on tissue factor (TF) and TF pathway inhibitor (TFPI) expression, an important component of endothelial dysfunction and consequently coagulation, has not been defined.

The activation of coagulation plays an important role in thrombus formation, which triggers acute coronary artery disease (13) and sepsis-associated disseminated intravascular coagulation syndrome (14). Initiation of coagulation occurs when blood is exposed to cells expressing TF. TF is a physiological constituent of subendothelial layers of blood vessels and perivascular tissues, forming a protective hemostatic lining that limits bleeding after vessel injury (15). Unlike resting endothelial cells, activated endothelial cells can also express TF (16, 17). TF binds and activates factor VII, leading to activation of factor X and ultimately to thrombin formation. Elevated TF expression has been detected in human coronary artery atheromas (18) and in septic organs (14, 19, 20). TF-initiated coagulation is under the control of TFPI, a Kunitz-type serine protease inhibitor, which forms a stable complex with TF/factor VIIa thereby preventing factor X activation (21). TFPI is predominantly produced by endothelial cells (22). Genetic deletion of TF in mice resulted in reduced coagulation and mortality in response to lipopolysaccharide (LPS) (23, 24). Inhibition of TF with recombinant TFPI or local gene transfer of TFPI reduced acute thrombus formation in human plaques (25), inhibited coagulation in experimental models of arterial injury (26, 27), and *Escherichia coli* sepsis (28).

In this study, we investigated the effects of CpG DNA on TF and TFPI expression in human coronary artery endothelial cells (HCAECs) and on coagulation in mice. We report that CpG DNA signaling through TLR9 alters the balance of TF and TFPI in HCAECs, consistent with a potent procoagulant action, and activates coagulation in wild type, but not in TLR9-deficient mice. We also show that these actions of CpG DNA can effectively be inhibited by a TLR9 inhibitory oligodeoxynucleotide.

MATERIALS AND METHODS

Bacterial and Mammalian DNA
Purified, heat-denaturated (single-stranded) *E. coli* DNA (strain B), methylated *E. coli* DNA, and calf thymus DNA (Sigma-Aldrich, Mississauga, ON, Canada) were used in all experiments (9). DNA preparations contained less than 5 ng LPS/mg DNA by Limulus assay (Sigma-Aldrich).

Culture and Stimulation of HCAECs
Primary HCAECs (Lonza, Walkersville, MD) were cultured in EGM-MV SingleQuots medium (Lonza). HCAECs (passages 4–6) were challenged with CpG DNA (0–16 μg/mL), methylated CpG DNA, or thymus DNA (both at 16 μg/mL). In some experiments, HCAECs were preincubated with a human

TLR9 inhibitory phosphorothioate oligodeoxynucleotide (iODN, 20 μmol/L; InvivoGen, San Diego, CA) (29), a negative control oligodeoxynucleotide (ODN) (2.4 μmol/L, InvivoGen), or the selective nuclear factor (NF)-κB inhibitors SN50 (4 μmol/L) or BAY 11–7082 (10 μmol/L; Calbiochem-EMD Biosciences, La Jolla, CA) for 20 minutes before addition of CpG DNA. At the indicated times, conditioned media were collected, and HCAECs were processed for subsequent analyses.

Culture of Human Peripheral Blood Monocytes
Peripheral blood mononuclear cells (PBMCs) (5×10^6 cells/mL), isolated from the venous blood of healthy volunteers (9), were challenged with CpG DNA (0–8 μg/mL) or thymus DNA (8 μg/mL) for 8 hours. The Clinical Research Committee at the Maisonneuve-Rosemont Hospital has approved the experimental protocols, and we obtained written consent from each blood donor.

TLR9 Expression
Lysates of HCAECs (passages 4 and 5) and PBMCs were subjected to Western blotting using a rabbit anti-human-TLR9 polyclonal antibody (Epitomics, Burlingame, CA) (9). To assess TLR9 location, untreated HCAECs were detached, permeabilized, and stained with R-PE-conjugated anti-TLR9 monoclonal antibody eB72-1665 or a class-matched irrelevant antibody (eBioscience, San Diego, CA). Fluorescence was assessed with a FACSCalibur flow cytometer and CellQuest software (BD Biosciences, Mountain View, CA) (9).

Measurement of Cellular and Secreted TF and TFPI Proteins
The culture supernatants were collected, and HCAECs and PBMCs were lysed in 100 μL of extraction buffer (50 mmol/L Tris, 100 mmo/L NaCl, 0.1% [w/vol] Triton X-100, pH 7.4). TF and TFPI levels were determined by IMUBIND Tissue Factor enzyme-linked immunosorbent assay (ELISA) and IMUBIND TFPI ELISA, respectively (American Diagnostica, Stamford, CT), and expressed as ng/mg protein. Intra-assay and inter-assay coefficients of variation were less than 7%.

TF and TFPI Activity Assays
TF and TFPI activity in conditioned culture medium were determined by the Actichrome TF and Actichrome TFPI activity assay kits, respectively (American Diagnostica). Intra-assay and inter-assay coefficients of variation were less than 8%.

For cell surface TF or TFPI activity, HCAECs were challenged for 8 and 24 hours, washed, and reagents were added directly to the microplate wells. To ascertain the specificity of the Actichrome TF assay (30), in some experiments, a function blocking mouse anti-human TF monoclonal antibody (10 μg/mL; Sekisui Diagnostics, Stamford, CT) was added to HCAECs, or factor VIIa was omitted from the assay. Intra-assay coefficients of variation were less than 6%.

TF and TFPI Gene Expression
Total RNA isolated from 5×10^5 HCAECs using TRIzol reagent (Invitrogen, Carlsbad, CA) was reverse transcribed into cDNA

using Superscript III reverse transcriptase (Invitrogen). Quantitative real-time polymerase chain reaction (qRT-PCR) was performed on an ABI 7500 Sequence Detection System (Applied Biosystems, Foster City, CA) using Platinum SYBR Green Super Mix (Invitrogen). Primer sequences are listed in **supplemental methods** (Supplemental Digital Content 1, http://links.lww.com/CCM/B275). Relative quantification was performed by the ΔΔCt method using 18s rRNA as endogenous control. TF and TFPI values were expressed as fold differences over control (unstimulated).

TLR9 Knockdown With Small Interfering RNA

HCAECs at ~40% confluence were transfected with small interfering RNA (siRNA) SR310036A or SR310036C targeted against TLR9 (10 nmol/L, hereafter referred to as siRNA1 and siRNA2, respectively) or scrambled negative control siRNA (SR30004; Origene Technologies, Rockville, MD) using DharmaFECT 4 transfection reagent (Thermo Scientific, Rockford, IL) for 6 hours. HCAECs were cultured in EGM-MV medium for an additional 48 hours. TLR9 expression was assessed as described above. Transfected HCAECs were challenged with CpG DNA (8 μg/mL) for 8 hours and lysed, and cellular TF protein levels were measured.

Nuclear Factor-κB Activation

Nuclear and cytoplasmic fractions were prepared from 5×10^5 HCAECs with the NE-PER Nuclear and Cytoplasmic Extraction kit (Thermo Scientific). Binding of NF-κB/p65 to the immobilized κB consensus sequence 5′-GGGACTTTCC-3′ was assayed with the TransAM NF-κB/p65 Activation Assay (Active Motif, Carlsbad, CA) using 5-μg nuclear extracts (9). Phosphorylation of I-κBα in cytosolic fractions was monitored with an ELISA kit (Invitrogen).

Western Blotting

Protein extracts prepared from 2.5×10^5 HCAECs or PBMCs were resolved by sodium dodecyl sulfate polyacrylamide gel electrophoresis, transferred to polyvinylidene difluoride membranes, and probed with antibodies to TF, phosphorylated extracellular signal-activated protein kinase 1/2 (ERK1/2), Akt, and p38 mitogen-activated protein kinase (MAPK) (Cell Signaling Technologies, Danvers, MA) (9).

Assessment of Coagulation In Vivo

Studies were performed on 5- to 7-week-old TLR9$^{-/-}$ mice (breeding pairs obtained from Dr. Akiko Iwasaki, Yale School of Medicine) (31) and wild-type C57BL/6 mice (Charles River Laboratories, St. Constant, QC, Canada) served as controls. The Animal Care Committee of the Maisonneuve-Rosemont Hospital approved the protocols. Mice were injected with CpG DNA or thymus DNA (0.25 or 1 μg/g body weight in 200 μL sterile saline, intraperitoneal) or saline as a control. Some mice were treated with iODN or control ODN (5 μg/g body weight, intraperitoneal) or a rat anti-mouse TF monoclonal antibody (Genentech, South San Francisco, CA clone 1H1, 20 μg/g body weight, IV) (32) or isotype-matched rat IgG2a (BD Biosciences)

20 minutes before injection of CpG DNA. To deplete blood monocytes, mice were injected with clodronate (dichloro-methylene-bisphosphonate)-loaded liposomes (VU Medical Centre, Amsterdam, The Netherlands; 50 μg clodronate/g body weight, IV) (33) or control liposomes 24 hours before injection of CpG DNA. Bleeding time was assessed at 6 and 24 hours post-CpG DNA injection (34). At the end of the assay, under isoflurane anesthesia, blood was collected by cardiac puncture. Blood monocyte count was determined following lysis of RBCs and staining with neutral red. Plasma was analyzed for thrombin-antithrombin (TAT) complexes using AssayMax mouse ELISA (AssayPro, St. Charles, MO). The intra-assay and inter-assay coefficients of variation were less than 5% and 7%, respectively. Plasma TF levels were measured with an ELISA (Biomatik, Cambridge, ON, Canada). Intra-assay coefficient of variation was less than 10%.

Immunohistochemical Staining for TF

Female C57BL/6 mice were killed at 6 hours post-CpG DNA injection. The heart and lungs were removed, fixed in 4% formaldehyde, and processed for histological analysis (35). Immunohistochemical detection was done with a Discovery XT immunostainer (Ventana Medical Systems, Tucson, AZ) using a rabbit anti-mouse TF antibody (Sekisui Diagnostics) followed by a biotinylated anti-rabbit IgG (Vector Laboratories, Burlingame, CA) and an anti-avidin-biotin-peroxidase system. The reaction products were stained with DAB substrate kit (DABmap kit; Ventana Medical Systems). Slides were counterstained with hematoxylin, scanned, and visualized using the C9600 NanoZoomer System (Hamamatsu Photonics K.K., Hamamatsu, Japan). Digital pictures were taken to illustrate antibody localization.

For details, see **supplemental data** (Supplemental Digital Content 1, http://links.lww.com/CCM/B275).

Statistical Analysis

Data are expressed as mean ± SEM. Statistical comparisons were made by analysis of variance using ranks followed by Dunn multiple contrast hypothesis tests or by the Mann-Whitney U test (two-tailed). p Values of less than 0.05 were considered statistically significant.

RESULTS

TLR9 Expression in HCAEC

By Western blot analysis, we found that HCAECs constitutively express TLR9 at high levels (**Fig. 1A**). TLR9 expression was confirmed with intracellular flow cytometry using permeabilized HCAECs (**Fig. 1B**). No specific signal was detected when nonpermeabilized HCAECs were stained with the anti-TLR9 antibody (Fig. 1B).

CpG DNA Induces TF and Suppresses TFPI Expression in HCAEC

To investigate the impact of CpG DNA on endothelial procoagulation, HCAECs were cultured up to 48 hours, and cellular expression and secretion of TF and TFPI were monitored. Culture of HCAECs with 8 μg/mL CpG DNA for 4 hours
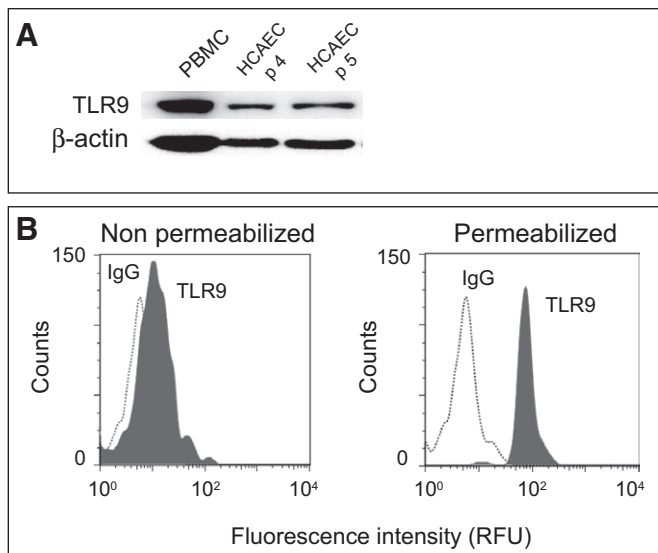
Figure 1. Toll-like receptor (TLR) 9 expression in human coronary artery endothelial cells (HCAECs). **A**, HCAEC (passages 4 and 5) lysates were subjected to immunoblotting with anti-TLR9 polyclonal antibody. Human peripheral blood mononuclear cell (PBMC) lysates served as positive controls. **B**, Intracellular localization of TLR9. Following detachment, nonpermeabilized and permeabilized HCAECs (passage 4) were stained with R-PE-conjugated anti-human TLR9 mAb eB72-1665 or its isotype control (IgG). Immunostaining was analyzed by flow cytometry. The results are representative of three determinations. RFU = relative fluorescence intensity units.

evoked marked increases in cellular TF protein, which peaked at 8 hours and remained elevated even after 48 hours of culture (**Fig. 2A**). The effects of CpG DNA were concentration dependent as assessed at 8 hours of culture (**Fig. 2B**). Unlike CpG DNA, methylated CpG DNA and calf thymus DNA did not induce TF expression (Fig. 2B). CpG DNA produced concentration-dependent increases in TF secretion, whereas methylated CpG DNA or calf thymus DNA were without effect (**Fig. 2C**). qRT-PCR confirmed CpG DNA induction of TF gene transcription in a time- and concentration-dependent manner (**Fig. 2D**). CpG DNA also increased TF expression in human PBMCs (**Fig. 2E**). CpG DNA induction of TF expression was confirmed by Western blotting (**Fig. S1**, Supplemental Digital Content 2, http://links.lww.com/CCM/B276)

CpG DNA induced decreases in cellular TFPI expression, and these changes became statistically significant after 24 hours of culture (**Fig. 2F**). The inhibitory action of CpG DNA was concentration dependent, and neither methylated CpG DNA nor thymus DNA mimicked the inhibitory action of CpG DNA (**Fig. 2G**). Consistently, CpG DNA attenuated TFPI levels in culture media in a concentration-dependent manner (**Fig. 2H**). qRT-PCR confirmed concentration-dependent suppression of TFPI gene transcription following 24-hour culture with CpG DNA (**Fig. 2I**).

CpG DNA Modulation of TF and TFPI Activity
Next, we investigated TF and TFPI activity levels as these are crucial for the regulation of the coagulation cascade. Culture of HCAECs for 8 hours with CpG DNA, but not with methylated CpG DNA or thymus DNA, dramatically enhanced TF

activity on the surface of HCAECs (**Fig. 3A**). Similar increases were detected in the conditioned culture media (**Fig. 3B**). No TF activity was detected in the presence of an anti-TF antibody or when factor VIIa was omitted, confirming the specificity of this assay (**Fig. S2**, Supplemental Digital Content 3, http://links.lww.com/CCM/B277). Conversely, culture of HCAECs with CpG DNA for 24 hours resulted in significant decreases in cell surface and culture media TFPI activity (**Fig 3, C** and **D**).

TLR9 Inhibition Prevents CpG DNA Effects
To assess the involvement of TLR9 in mediating the actions of CpG DNA on HCAECs, we used a TLR9 inhibitory ODN (29) and knocked down TLR9 with siRNA. Pretreatment of HCAECs with 20 μM iODN efficiently prevented CpG DNA induction of cellular TF expression (**Fig. 4A**) or suppression of TFPI (**Fig. 4B**). The control ODN was without detectable effects (Fig. 4, A and B).

To confirm the results with iODN, we used siRNA to transiently knockdown TLR9 in HCAECs. Two siRNA constructs designated siRNA1 and siRNA2, produced ~40% reductions in TLR9 protein expression assessed by flow cytometry (**Fig. 4C**), and confirmed by Western blotting and densitometry analysis (**Fig. 4D**). Consistent with partial TLR9 knockdown, siRNA1 and siRNA2 attenuated ~40% of CpG DNA-induced cellular TF protein expression (**Fig. 4E**). Transfection with a scrambled control siRNA neither affected TLR9 expression (Fig. 4, C and D) nor HCAEC responses to CpG DNA (Fig. 4E).

To further probe the mechanisms underlying CpG DNA induction of TF, we studied the activation of the MAPK and NF-κB pathways and used selective pharmacological inhibitors of these pathways. CpG DNA evoked rapid phosphorylation of cytoplasmic IκB-α, which was associated with increases in binding of nuclear extracts to immobilized κB consensus sequence, indicating increased nuclear accumulation of NF-κB (**Fig. 5A**). These actions were concentration dependent (**Fig. 5B**). Statistically significant changes were detected with 2 μg/mL CpG DNA. Preincubation of HCAECs with the NF-κB inhibitors BAY 11–7089 or SN50 inhibited 67–88% of CpG DNA-induced cellular TF protein expression (**Fig. 5C**) and cell surface TF activity (**Fig. 5D**), whereas they did not reverse CpG DNA suppression of TFPI expression (**Fig. S3**, Supplemental Digital Content 4, http://links.lww.com/CCM/B278). CpG DNA also evoked phosphorylation of p38 MAPK, ERK1/2, and Akt (**Fig. S4**, Supplemental Digital Content 5, http://links.lww.com/CCM/B279). The phosphoinositide 3-kinase (PI3K) inhibitor wortmannin further enhanced TF induction by CpG DNA, whereas pharmacological blockade of p38 MAPK and ERK1/2 did not produce statistically significant changes in HCAEC responses to CpG DNA (Fig. S4, Supplemental Digital Content 5, http://links.lww.com/CCM/B279).

CpG DNA Activates In Vivo Coagulation
Having shown opposing regulation of TF and TFPI expression by endothelial cells in vitro, we compared the effects of CpG DNA on bleeding time and plasma levels of TAT complexes as surrogate markers of blood coagulation activation in mice. Single
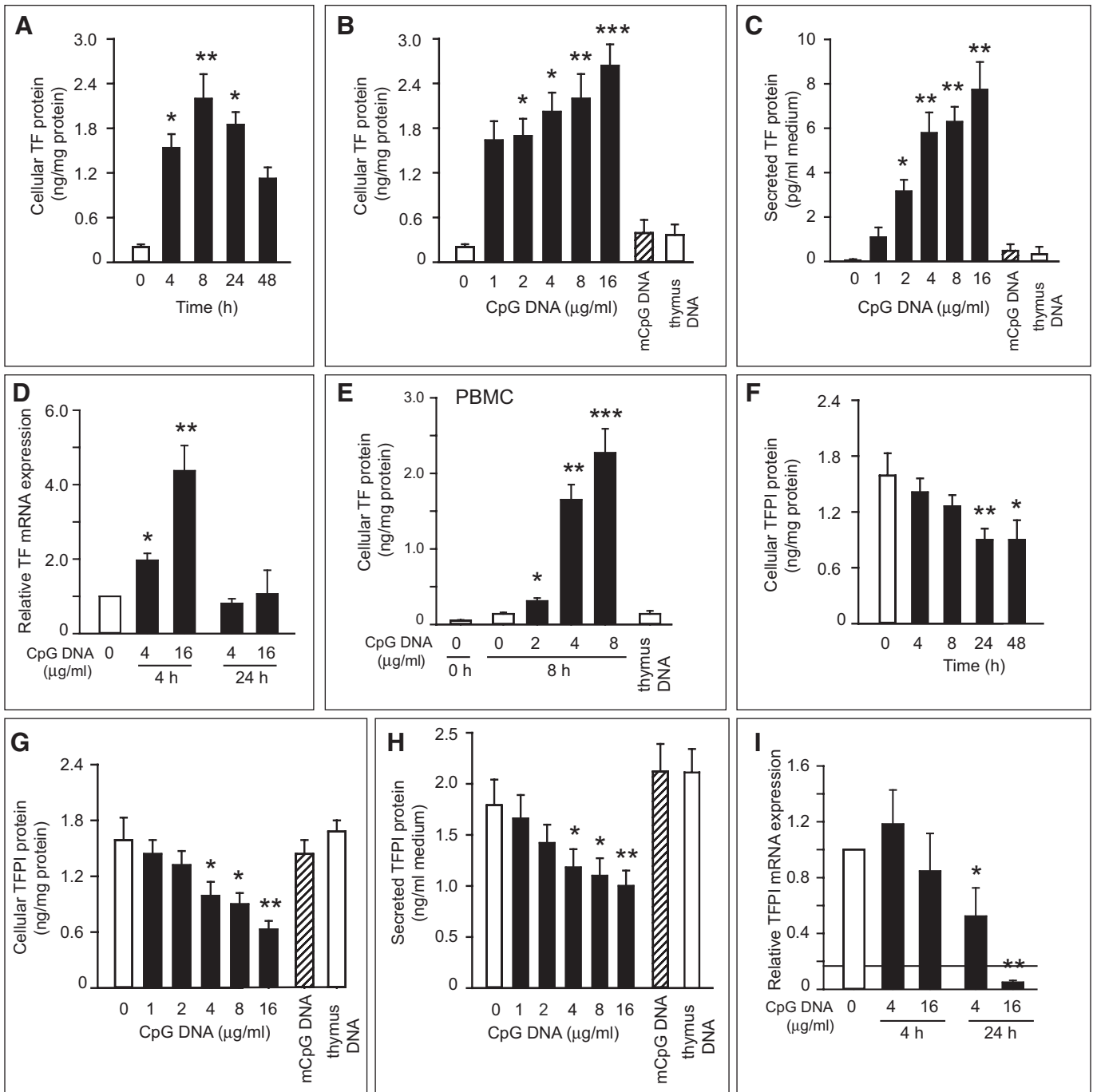
Figure 2. CpG DNA induces tissue factor (TF) expression and suppresses TF pathway inhibitor (TFPI) expression in human coronary artery endothelial cells (HCAECs). Confluent HCAEC monolayers were cultured with CpG DNA, methylated CpG DNA (mCpG DNA), or thymus DNA (all at 8 µg/mL) for 8 hr (TF protein analysis), 24 hr (TFPI protein analysis), or in a time course. **A**, CpG DNA (8 µg/mL) increases cellular TF protein level. Concentration-dependent effects of CpG DNA on cellular TF protein (**B**) and TF secretion into culture medium (**C**). **D**, CpG DNA-induced TF messenger RNA (mRNA) expression. **E**, CpG DNA-induced TF expression in human peripheral blood mononuclear cells (PBMCs). **F–I**, CpG DNA suppresses TFPI protein and mRNA expression. Time (F) and concentration-dependent changes in cellular TFPI level (G). H, TFPI protein levels in culture media. I, TFPI mRNA expression. The results are mean ± SEM ($n = 3$–6). $*p < 0.05$, $**p < 0.01$, $***p < 0.001$ versus 0 (vehicle control).

intraperitoneal injection of CpG DNA into female wild-type mice dramatically shortened bleeding time assessed at 6 hours postinjection (**Fig. 6A**). Significantly reduced bleeding time was still detectable at 24 hours postinjection (**Fig. 6B**). These changes coincided with increases in plasma levels of TAT (Fig. 6, *A* and *B*) and TF (**Fig. 6D**). The effects of CpG DNA were dose dependent

(Fig. 6*A*). Pretreatment with iODN rendered the mice unresponsive to CpG DNA (Fig. 6*A*). Neither iODN alone nor thymus DNA evoked detectable changes in bleeding time and plasma TAT level (Fig. 6*A*). Bleeding time and baseline plasma TAT levels did not differ in wild-type and TLR9-deficient female (**Fig. 6C**) and male mice (**Fig. S5**, Supplemental Digital Content 6, http://
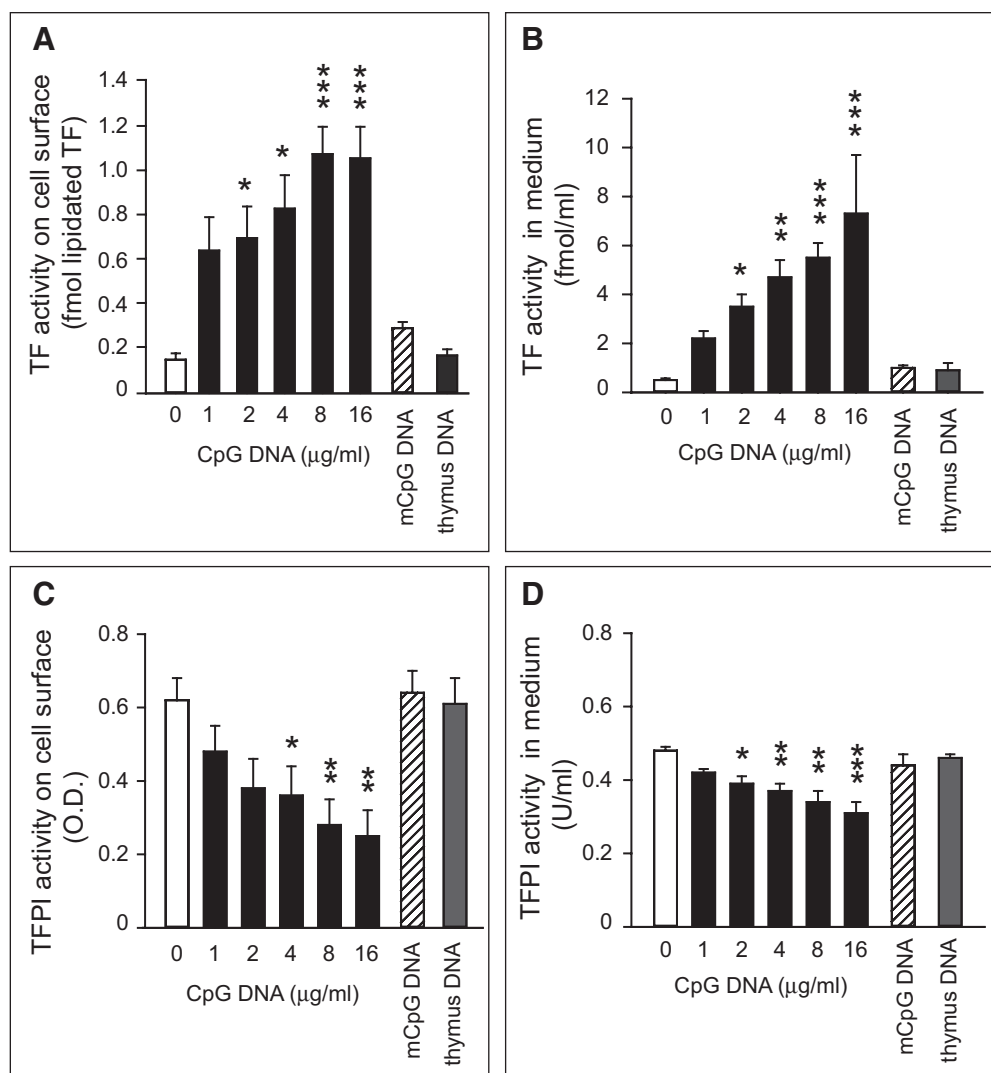
Figure 3. CpG DNA induces tissue factor (TF) activity and decreases TF pathway inhibitor (TFPI) activity. Human coronary artery endothelial cells were cultured with CpG DNA, methylated CpG DNA (mCpG DNA), or thymus DNA (all at 8 μg/mL) for 8 hr (TF activity) or for 24 hr (TFPI activity). TF activity on cell surface (**A**) and culture medium (**B**). TFPI activity on cell surface (**C**) and culture medium (**D**). The results are mean ± SEM ($n = 6$). $^*p < 0.05$, $^{**}p < 0.01$, $^{***}p < 0.001$ versus 0 (vehicle control).

DISCUSSION

In this study, we have demonstrated that bacterial DNA is a potent and highly efficacious activator of coagulation. CpG DNA was intimately associated with activation of HCAECs, resulting in a procoagulant phenotype in HCAECs by inducing TF transcription, expression, and activity and suppressing the expression and activity of TFPI. Consistently, CpG DNA activated coagulation in mice as evidenced by shortened bleeding time and elevated plasma levels of TAT complexes and TF. These changes were only partially prevented by depleting of blood monocytes.

Consistent with earlier findings on venous, microvascular, and lymphatic endothelial cells (9–11), we found that primary HCAECs also express functional TLR9. Using permeabilized cells and flow cytometry, we confirmed intracellular location of TLR9. We did not detect specific staining for TLR9 on nonpermeabilized HCAECs. Our results indicate that differences in DNA methylation patterns enabled HCAECs to recognize and selectively respond to CpG DNA, for methylating cytosines in CpG dinucleotides resulted in complete loss of its biological activities. Furthermore, thymus DNA did not reproduce the actions of CpG DNA. CpG motifs are commonly methylated in eukaryotic DNA, and inhibitory sequences flanking CpG dinucleotides in mammalian DNA can also mask its stimulatory effects (36).

Previous studies demonstrated that endothelial cells activated by mediators implicated in coronary artery disease and sepsis, including LPS (16, 37), tumor necrosis factor (TNF)-α (38), C-reactive protein (39), and serum amyloid A (40) express TF. Our results show that CpG DNA can also induce TF expression in HCAECs, and this was confirmed at the messenger RNA (mRNA), protein, and activity levels. CpG DNA-induced TF levels in HCAECs were comparable to those detected in PBMCs. The effects of CpG DNA were rapid in onset, peaking at around 8 hours, and the magnitude of responses was comparable to that of TNF-α (38) and serum amyloid A (40).

links.lww.com/CCM/B280). In contrast to wild-type mice, injection of CpG DNA into TLR9-deficient mice did not shorten bleeding time and did not evoke increases in plasma TAT and TF levels (Fig. 6, *C* and *D*; and Fig. S5, Supplemental Digital Content 6, http://links.lww.com/CCM/B280), indicating lack of activation of coagulation. Likewise, pretreatment with an anti-mouse TF antibody (32) abolished the effects of CpG DNA (Fig. 6*C*). As anticipated (33), treatment of mice with clodronate-containing liposomes reduced circulating monocyte number by about 80% (**Fig. 7A**). This was associated with prolonged bleeding time and slight decreases in plasma TAT levels (**Fig. 7, *B* and *C***). Injection of CpG DNA to monocyte-depleted mice effectively shortened bleeding time and markedly increased plasma TAT levels (Fig. 7, *B* and *C*). Furthermore, CpG DNA enhanced TF staining of endothelial cells in the heart and lung (**Fig. S6**, Supplemental Digital Content 7, http://links.lww.com/CCM/B281).
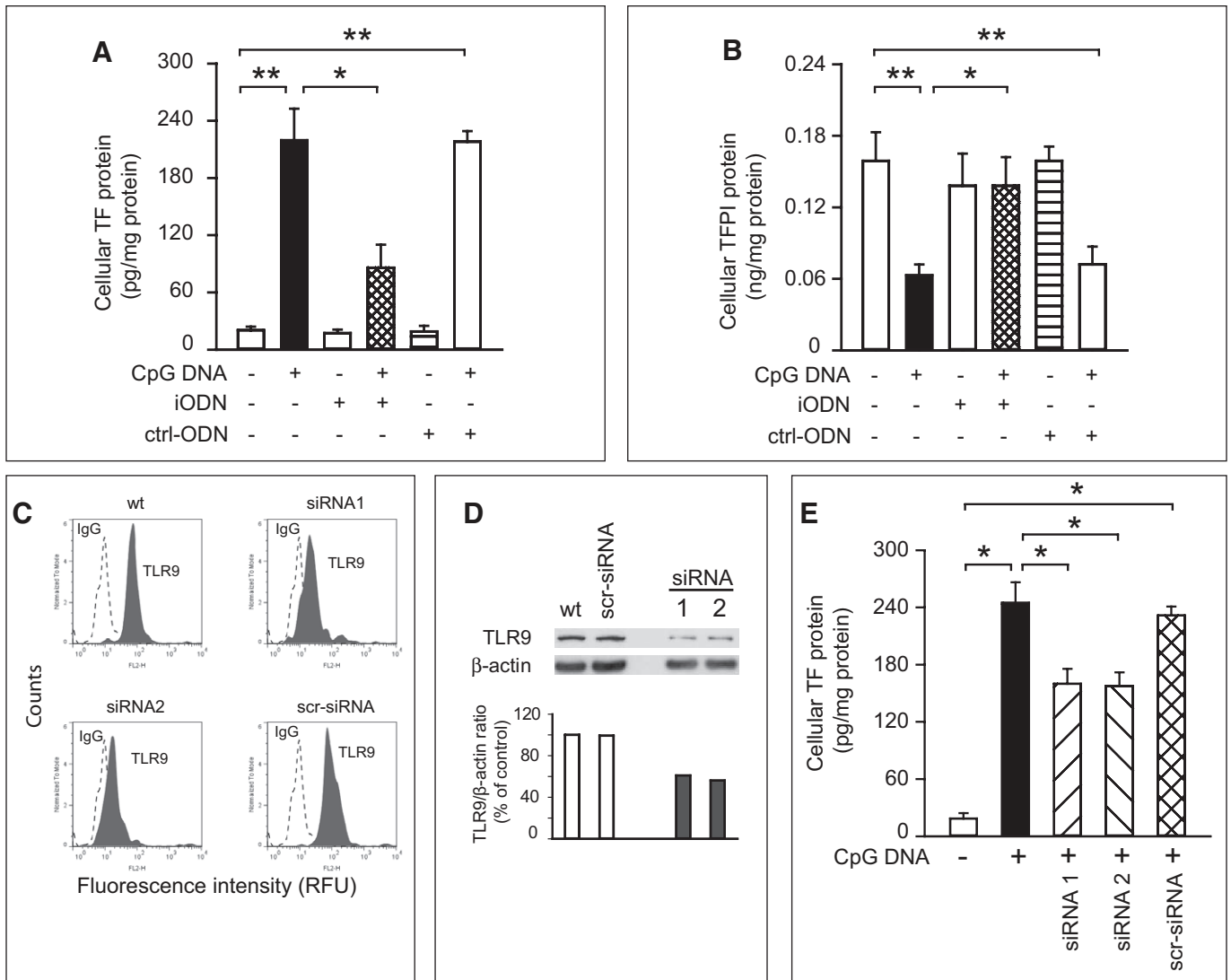
Figure 4. Toll-like receptor (TLR) 9 inhibition attenuates CpG DNA-induced tissue factor (TF) expression and reduction of TF pathway inhibitor (TFPI) expression in human coronary artery endothelial cells (HCAECs). **A** and **B**, HCAECs were cultured with CpG DNA (8 μg/mL) in the presence of inhibitory oligonucleotide (iODN) (20 μmol/L) or control ODN (ctrl-ODN, 20 μmol/L) for 8 and 24 hr for detection of cellular TF (A) and TFPI levels (B), respectively. **C** and **D**, Transient knockdown of TLR9 with siRNA. HCAECs were transfected with anti-TLR9 siRNA1 or siRNA2 or a scrambled siRNA (scr-siRNA). TLR9 expression was assessed with intracellular flow cytometry (C) and Western blotting (D, upper panel: Western blot; lower panel: densitometry analysis). Following detachment, transfected HCAECs were permeabilized and stained with R-PE-conjugated anti-human TLR9 monoclonal antibody eB72-1665 or its isotype control (IgG) or were lysed and subjected to immunoblotting with an anti-TLR9 polyclonal antibody. Results are representative of three independent experiments. **E**, Attenuation of CpG-DNA induced cellular TF protein expression. Nontransfected and transfected HCAECs were cultured with CpG DNA for 8 hr. The results are mean ± SEM ($n = 3$–6). $*p < 0.05$, $**p < 0.01$. RFU = relative fluorescence units, wt = wild type.

However, unlike these mediators, CpG DNA-induced TF protein expression remained significantly elevated at 24 hours. Release of TF protein and activity into the culture medium would suggest that in addition to expressing active TF on their surface, HCAECs may contribute to functionally active TF circulating in blood. We also detected markedly elevated plasma TF levels in response to CpG DNA in mice. Additional studies are required to investigate whether TF was contained in microparticles or was present in soluble form.

TFPI is attached to the endothelium via proteoglycans and regulates TF expression and activity (21). Studies on TFPI expression in situations of TF-induced coagulation have yielded inconsistent results. LPS and TNF-α, but not IL-1, were reported to decrease TFPI mRNA in murine endothelial cells (41). TNF-α was found to decrease TFPI protein in HUVEC lysates, while it increased TFPI secretion (42). Increases in plasma TFPI activity in meningococcal sepsis portend more severe coagulation and increased mortality (43), suggesting that TFPI may work less efficiently when it is not attached to endothelial cells. Our data demonstrate that CpG DNA evoked simultaneous decreases in both cellular and secreted TFPI protein levels and activity, indicating that these effects were a consequence of reduced protein synthesis and cannot be attributed to enhanced TFPI secretion or a direct inhibition of TFPI activity. Our mRNA results confirmed the ability of CpG DNA to suppress *TFPI* transcription. CpG DNA shifted the balance of TF and TFPI toward a
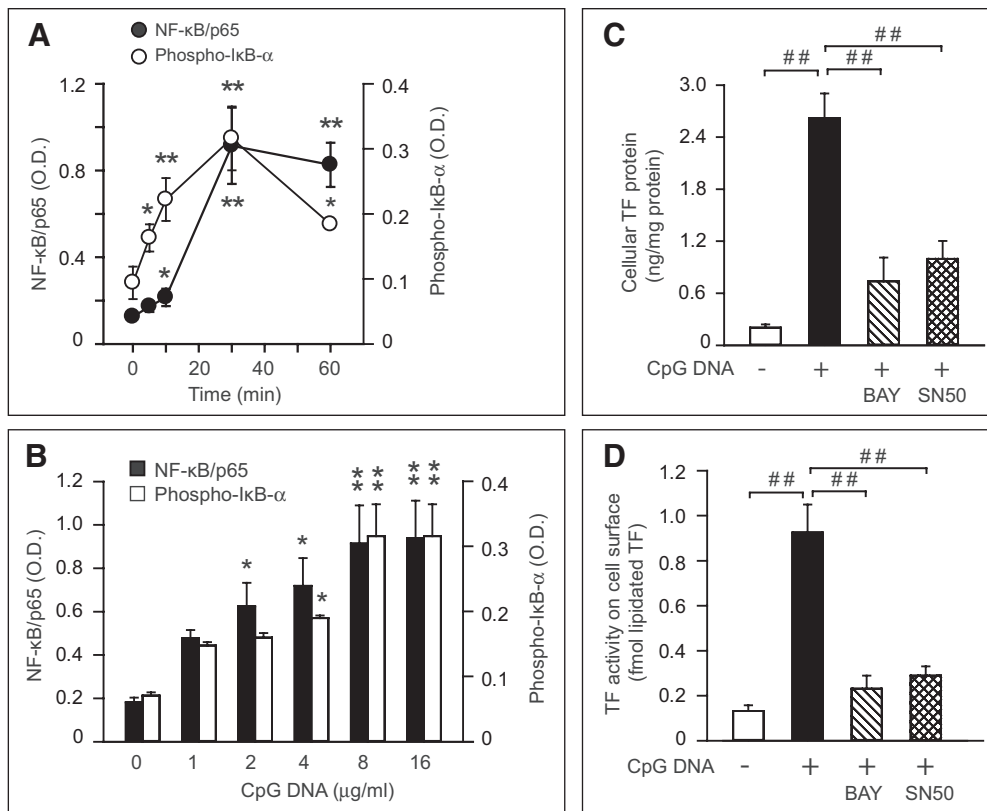
Figure 5. CpG DNA-induced tissue factor (TF) expression is mediated by nuclear factor (NF)-κB. Human coronary artery endothelial cell (HCAEC) monolayers were cultured for the indicated times with 8 μg/mL CpG DNA (**A**) or for 30 min with increasing concentrations of CpG DNA (**B**). Nuclear fractions were prepared, and DNA binding of NF-κB was detected by enzyme-linked immunosorbent assay (ELISA) using an immobilized κB consensus sequence and is expressed as optical density (O.D.). Binding was inhibited by more than 95% in the presence of 20 pmol wild-type NF-κB. Phosphorylation of IκB-α in the cytosolic fraction was monitored with ELISA and expressed as the O.D. **C** and **D**, NF-κB inhibitors attenuate CpG DNA-evoked increases in cellular TF protein level (C) and cell surface TF activity (D). HCAECs were cultured with CpG DNA (8 μg/mL) in the presence of BAY 11−7082 (BAY, 10 μmol/L) or SN50 (4 μmol/L) for 8 hr. The results are mean ± SEM ($n = 4$–6). $^*p < 0.05$, $^{**}p < 0.01$ versus 0 (control). $^{##}p < 0.01$.

CpG DNA binding to TLR9 triggers MyD88-mediated activation of the canonical NF-κB pathway and MAPK pathways (44). We detected rapid nuclear accumulation and DNA binding of NF-κB/p65 in HCAECs in response to CpG DNA. Pharmacological blockade of NF-κB produced almost complete inhibition of CpG DNA-stimulated TF protein expression and activity. CpG DNA also evoked phosphorylation of Akt, p38 MAPK, and ERK1/2. PI3K inhibition enhanced CpG DNA-stimulated TF expression, whereas pharmacological blockade of the other pathways had no significant effects. These findings indicate a predominant role for TLR9/NF-κB-mediated signaling in inducing TF gene transcription, protein expression, and activity, which is regulated by a PI3K-mediated negative feedback signal. By contrast, in macrophages, TLR9 activation with a synthetic oligodeoxynucleotide was found to stimulate TF mRNA expression through the MyD88-ERK1/2-Egr-1 pathway (45),

procoagulant state in HCAECs. Thus, at 4 and 8 hours of culture CpG DNA-evoked dramatic increases in TF transcription, protein expression and activity were associated with moderate decreases in TFPI protein and activity. This procoagulant state persisted for at least 48 hours despite declining TF level due to further decreases in TFPI expression and activity. CpG DNA-induced procoagulant state in HCAECs may have relevance to triggering acute coronary events since CpG DNA is present in human coronary arteries (5), and endothelial cells of human atherosclerotic plaques express TLR9 (12).

Loss of biological activities in methylated CpG DNA and the inability of thymus DNA to activate HCAECs implied involvement of TLR9 in CpG DNA-evoked HCAEC responses. This was confirmed with transfection of HCAECs with TLR9 siRNA, which resulted in parallel decreases in TLR9 and TF protein expression. Furthermore, the effects of CpG DNA were effectively inhibited by a telomere-derived iODN. This iODN contains the potent TLR9 inhibitory sequence TTAGGG multimers, diffuses freely into cells, and disrupts interaction of CpG DNA with TLR9 in endosomal vesicles without affecting cellular uptake of CpG DNA (29).

indicating cell type-specific TLR9 signaling to regulate TF gene transcription. Our results also confirmed involvement of TLR9 in mediating CpG DNA-evoked decreases in TFPI protein and activity. These likely occurred through inhibition of TFPI gene expression, as supported by our mRNA results. Of note, recent data suggest that TLR9-independent cytosolic DNA sensors, such as DNA-dependent activator of interferon-regulatory factors (or DLM-1/Z-DNA binding protein 1) or absent in melanoma-2 can activate innate immunity to endogenous DNA that escaped lysosomal degradation (46, 47). However, the expression and function of such sensors in HCAECs remain to be investigated.

Our results also document CpG DNA activation of blood coagulation in vivo. Indeed, single peritoneal injection of CpG DNA at pathologically relevant local concentrations (2) evoked marked reductions in bleeding time parallel with increases in plasma TAT complex and TF levels as assessed 6 hours after CpG DNA administration in wild-type mice. We detected significantly increased blood coagulation even 24 hours after CpG DNA injection. It remains to be investigated whether decreased availability of TFPI may inadequately
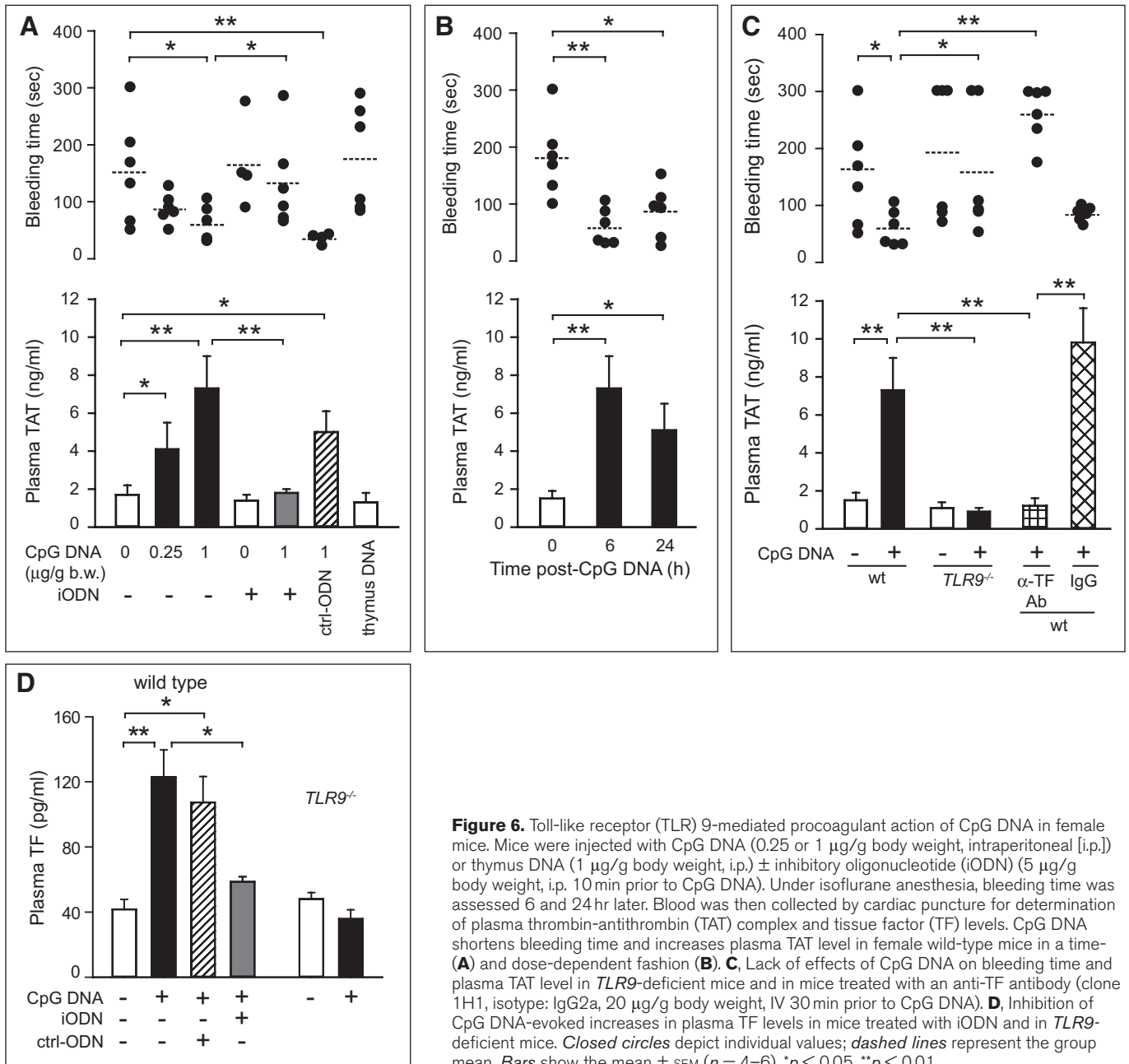
Figure 6. Toll-like receptor (TLR) 9-mediated procoagulant action of CpG DNA in female mice. Mice were injected with CpG DNA (0.25 or 1 μg/g body weight, intraperitoneal [i.p.]) or thymus DNA (1 μg/g body weight, i.p.) ± inhibitory oligonucleotide (iODN) (5 μg/g body weight, i.p. 10 min prior to CpG DNA). Under isoflurane anesthesia, bleeding time was assessed 6 and 24 hr later. Blood was then collected by cardiac puncture for determination of plasma thrombin-antithrombin (TAT) complex and tissue factor (TF) levels. CpG DNA shortens bleeding time and increases plasma TAT level in female wild-type mice in a time- (**A**) and dose-dependent fashion (**B**). **C**, Lack of effects of CpG DNA on bleeding time and plasma TAT level in *TLR9*-deficient mice and in mice treated with an anti-TF antibody (clone 1H1, isotype: IgG2a, 20 μg/g body weight, IV 30 min prior to CpG DNA). **D**, Inhibition of CpG DNA-evoked increases in plasma TF levels in mice treated with iODN and in *TLR9*-deficient mice. *Closed circles* depict individual values; *dashed lines* represent the group mean. *Bars* show the mean ± SEM (*n* = 4–6). *$p < 0.05$, **$p < 0.01$.

balance the increased TF-dependent coagulation and therefore perpetuates the procoagulant state, as suggested by our in vitro results. *E. coli*-induced septicemia in baboons is associated with significant reductions in TFPI anticoagulant activity in the lungs (20). Endothelial cells are predominant source (up to 90%) of the total intravascular pool of TFPI (22). Although we detected enhanced TF staining in endothelial cells in response to CpG DNA in vivo, our study provides limited information on the relative contribution of TF from various cell types to CpG DNA-stimulated activation of coagulation. We found that depletion of blood monocytes prolonged bleeding time in naïve mice, but only modestly attenuated the effects of CpG DNA, indicating that cells other than monocytes play

relatively dominant role CpG DNA-evoked coagulation disorder. In a mouse endotoxemia model, nonhematopoietic cells were found to contribute only about 50% of the TF-dependent activation of coagulation with modest contributions by endothelial and vascular smooth muscle cells (24). The identity of TF-generating nonhematopoietic cell type(s) and the impact of CpG DNA on these cells remain to be investigated. By contrast, endothelial cell-specific overexpression of a dominant negative IκBα attenuated endothelial TF expression within the renal vasculature and markedly reduced plasma TAT levels and inflammation in endotoxemic mice (48, 49). Intriguingly, endothelial cell-specific deletion of TF gene had little effect on plasma TAT level, whereas it reduced IL-6 level in mouse
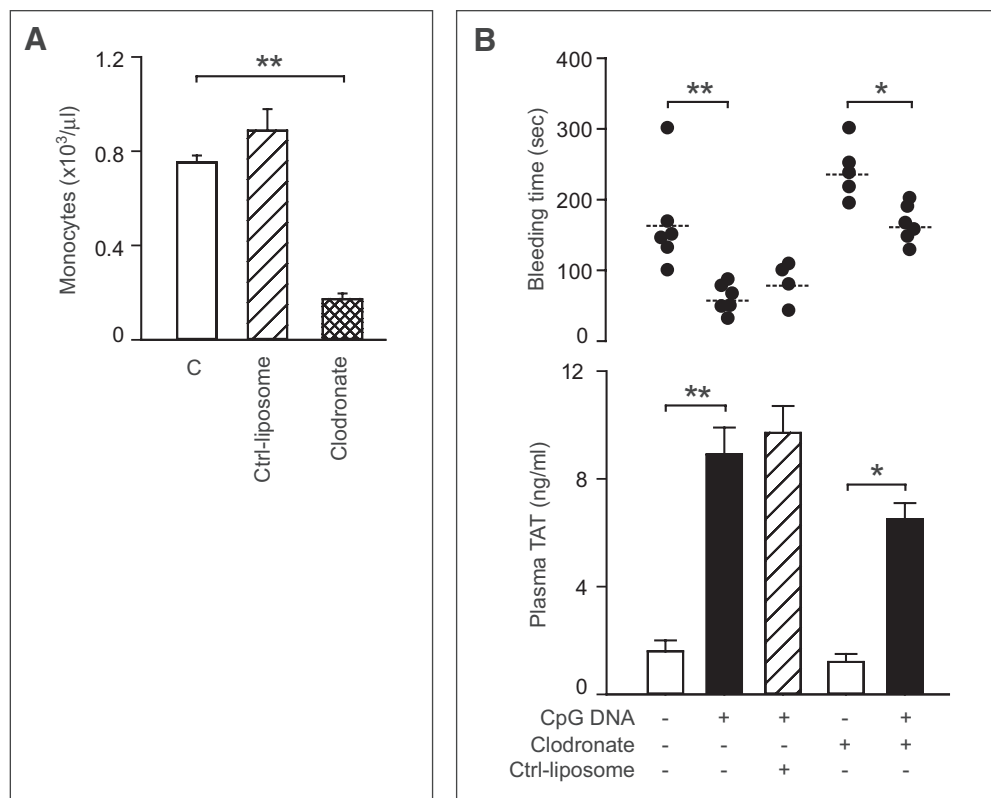
Figure 7. Procoagulant action of CpG DNA in monocyte-depleted mice. Female mice were treated with clodronate-loaded liposomes (clodronate, 50 µg/g body weight, IV) or control liposomes (ctrl-liposomes) for 24 hr before injection of CpG DNA (1 µg/g body weight, intraperitoneal). Bleeding time was assessed 6 hr later under isoflurane anesthesia. Blood was then collected by cardiac puncture for determination of plasma thrombin-antithrombin (TAT) complex levels. **A**, Depletion of blood monocytes by clodronate. **B**, CpG DNA evoked shortening of bleeding time and increases in plasma TAT. *Closed circles* depict individual values; *dashed lines* represent the group mean. *Bars* show the mean ± SEM ($n = 4–6$). $^{*}p < 0.05$, $^{**}p < 0.01$.

delineate the effects of CpG DNA on TF expression and activation of coagulation during bacterial infection and sepsis.

In summary, our results demonstrate that bacterial DNA, signaling through TLR9, induces TF expression and reduces TFPI expression in HCAECs and activates blood coagulation in mice. These finding suggest a role for CpG DNA to contribute to hypercoagulable state in the local and/or systemic circulation and identify TLR9 inhibitory oligonucleotides as potential novel therapeutic agents for the prevention of coagulation in pathologies, such as acute coronary artery diseases and sepsis, where bacterial DNA may abundantly be present.

models of sickle cell disease (50). These findings indicate a complex interplay between endothelial TF and inflammation to regulate coagulation and suggest context-dependent contribution of endothelial cells to TF expression.

Regardless of the cellular origins of TF in vivo, our results indicate a predominant role for TLR9 in mediating the procoagulant action of CpG DNA in mice. Thus, unlike CpG DNA, thymus DNA failed to activate coagulation and genetic deletion of TLR9 rendered mice unresponsive to CpG DNA. Consistent with our in vitro findings, telomere-derived iODN prevented the effects of CpG DNA on bleeding time and plasma TF and TAT complexes. Since CpG DNA also exerts potent proinflammatory actions, including facilitation of leukocyte trafficking (2, 9, 51, 52) and suppression of neutrophil apoptosis (53) predominantly through TLR9 (9, 51, 53), activation of this receptor may represent another link between inflammation and coagulation. Of note, TLR9 also binds endogenous ligands, including mitochondrial DNA released from damaged cells (4), lending further support to this notion. TLR9 signaling is also required for thrombus resolution in a model of stasis (54), illustrating the complex role of TLR9 signaling in thrombosis and coagulation. Additional studies with TLR9-deficient mice or iODN are required to

REFERENCES

1. Krieg AM, Yi AK, Matson S, et al: CpG motifs in bacterial DNA trigger direct B-cell activation. *Nature* 1995; 374:546–549

2. Schwartz DA, Quinn TJ, Thorne PS, et al: CpG motifs in bacterial DNA cause inflammation in the lower respiratory tract. *J Clin Invest* 1997; 100:68–73

3. Krieg AM: CpG motifs in bacterial DNA and their immune effects. *Annu Rev Immunol* 2002; 20:709–760

4. Zhang Q, Raoof M, Chen Y, et al: Circulating mitochondrial DAMPs cause inflammatory responses to injury. *Nature* 2010; 464:104–107

5. Lehtiniemi J, Karhunen PJ, Goebeler S, et al: Identification of different bacterial DNAs in human coronary arteries. *Eur J Clin Invest* 2005; 35:13–16

6. Ratanarat R, Cazzavillan S, Ricci Z, et al: Usefulness of a molecular strategy for the detection of bacterial DNA in patients with severe sepsis undergoing continuous renal replacement therapy. *Blood Purif* 2007; 25:106–111

7. Hemmi H, Takeuchi O, Kawai T, et al: A Toll-like receptor recognizes bacterial DNA. *Nature* 2000; 408:740–745

8. Akira S, Uematsu S, Takeuchi O: Pathogen recognition and innate immunity. *Cell* 2006; 124:783–801

9. El Kebir D, József L, Pan W, et al: Bacterial DNA activates endothelial cells and promotes neutrophil adherence through TLR9 signaling. *J Immunol* 2009; 182:4386–4394

10. Fitzner N, Clauberg S, Essmann F, et al: Human skin endothelial cells can express all 10 TLR genes and respond to respective ligands. *Clin Vaccine Immunol* 2008; 15:138–146

11. Pegu A, Qin S, Fallert Junecko BA, et al: Human lymphatic endothelial cells express multiple functional TLRs. *J Immunol* 2008; 180:3399–3405

12. Edfeldt K, Swedenborg J, Hansson GK, et al: Expression of toll-like receptors in human atherosclerotic lesions: A possible pathway for plaque activation. *Circulation* 2002; 105:1158–1161

13. Steffel J, Lüscher TF, Tanner FC: Tissue factor in cardiovascular diseases: Molecular mechanisms and clinical implications. *Circulation* 2006; 113:722–731

14. van der Poll T: Tissue factor as an initiator of coagulation and inflammation in the lung. *Crit Care* 2008; 12(Suppl 6):S3

15. Drake TA, Morrissey JH, Edgington TS: Selective cellular expression of tissue factor in human tissues. Implications for disorders of hemostasis and thrombosis. *Am J Pathol* 1989; 134:1087–1097

16. Colucci M, Balconi G, Lorenzet R, et al: Cultured human endothelial cells generate tissue factor in response to endotoxin. *J Clin Invest* 1983; 71:1893–1896

17. Parry GC, Mackman N: Transcriptional regulation of tissue factor expression in human endothelial cells. *Arterioscler Thromb Vasc Biol* 1995; 15:612–621

18. Marmur JD, Thiruvikraman SV, Fyfe BS, et al: Identification of active tissue factor in human coronary atheroma. *Circulation* 1996; 94:1226–1232

19. van Till JW, Levi M, Bresser P, et al: Early procoagulant shift in the bronchoalveolar compartment of patients with secondary peritonitis. *J Infect Dis* 2006; 194:1331–1339

20. Tang H, Ivanciu L, Popescu N, et al: Sepsis-induced coagulation in the baboon lung is associated with decreased tissue factor pathway inhibitor. *Am J Pathol* 2007; 171:1066–1077

21. Ott I, Miyagi Y, Miyazaki K, et al: Reversible regulation of tissue factor-induced coagulation by glycosyl phosphatidylinositol-anchored tissue factor pathway inhibitor. *Arterioscler Thromb Vasc Biol* 2000; 20:874–882

22. Crawley JT, Lane DA: The haemostatic role of tissue factor pathway inhibitor. *Arterioscler Thromb Vasc Biol* 2008; 28:233–242

23. Pawlinski R, Pedersen B, Schabbauer G, et al: Role of tissue factor and protease-activated receptors in a mouse model of endotoxemia. *Blood* 2004; 103:1342–1347

24. Pawlinski R, Wang JG, Owens AP 3rd, et al: Hematopoietic and non-hematopoietic cell tissue factor activates the coagulation cascade in endotoxemic mice. *Blood* 2010; 116:806–814

25. Badimon JJ, Lettino M, Toschi V, et al: Local inhibition of tissue factor reduces the thrombogenicity of disrupted human atherosclerotic plaques: Effects of tissue factor pathway inhibitor on plaque thrombogenicity under flow conditions. *Circulation* 1999; 99:1780–1787

26. Roqué M, Reis ED, Fuster V, et al: Inhibition of tissue factor reduces thrombus formation and intimal hyperplasia after porcine coronary angioplasty. *J Am Coll Cardiol* 2000; 36:2303–2310

27. Nishida T, Ueno H, Atsuchi N, et al: Adenovirus-mediated local expression of human tissue factor pathway inhibitor eliminates shear stress-induced recurrent thrombosis in the injured carotid artery of the rabbit. *Circ Res* 1999; 84:1446–1452

28. Creasey AA, Chang AC, Feigen L, et al: Tissue factor pathway inhibitor reduces mortality from *Escherichia coli* septic shock. *J Clin Invest* 1993; 91:2850–2860

29. Gursel I, Gursel M, Yamada H, et al: Repetitive elements in mammalian telomeres suppress bacterial DNA-induced immune activation. *J Immunol* 2003; 171:1393–1400

30. Bogdanov VY, Cimmino G, Tardos JG, et al: Assessment of plasma tissue factor activity in patients presenting with coronary artery disease: Limitations of a commercial assay. *J Thromb Haemost* 2009; 7:894–897

31. Lund J, Sato A, Akira S, et al: Toll-like receptor 9-mediated recognition of Herpes simplex virus-2 by plasmacytoid dendritic cells. *J Exp Med* 2003; 198:513–520

32. Kirchhofer D, Moran P, Bullens S, et al: A monoclonal antibody that inhibits mouse tissue factor function. *J Thromb Haemost* 2005; 3:1098–1099

33. Sunderkötter C, Nikolic T, Dillon MJ, et al: Subpopulations of mouse blood monocytes differ in maturation stage and inflammatory response. *J Immunol* 2004; 172:4410–4417

34. Schwarz M, Meade G, Stoll P, et al: Conformation-specific blockade of the integrin GPIIb/IIIa: A novel antiplatelet strategy that selectively targets activated platelets. *Circ Res* 2006; 99:25–33

35. Wang MY, Ji SR, Bai CJ, et al: A redox switch in C-reactive protein modulates activation of endothelial cells. *FASEB J* 2011; 25:3186–3196

36. Stacey KJ, Young GR, Clark F, et al: The molecular basis for the lack of immunostimulatory activity of vertebrate DNA. *J Immunol* 2003; 170:3614–3620

37. Wu SQ, Aird WC: Thrombin, TNF-alpha, and LPS exert overlapping but nonidentical effects on gene expression in endothelial cells and vascular smooth muscle cells. *Am J Physiol Heart Circ Physiol* 2005; 289:H873–H885

38. Steffel J, Hermann M, Greutert H, et al: Celecoxib decreases endothelial tissue factor expression through inhibition of c-Jun terminal NH2 kinase phosphorylation. *Circulation* 2005; 111:1685–1689

39. Cirillo P, Golino P, Calabrò P, et al: C-reactive protein induces tissue factor expression and promotes smooth muscle and endothelial cell proliferation. *Cardiovasc Res* 2005; 68:47–55

40. Zhao Y, Zhou S, Heng CK: Impact of serum amyloid A on tissue factor and tissue factor pathway inhibitor expression and activity in endothelial cells. *Arterioscler Thromb Vasc Biol* 2007; 27:1645–1650

41. Shimokawa T, Yamamoto K, Kojima T, et al: Down-regulation of murine tissue factor pathway inhibitor mRNA by endotoxin and tumor necrosis factor-alpha in vitro and in vivo. *Thromb Res* 2000; 100:211–221

42. Szotowski B, Antoniak S, Poller W, et al: Procoagulant soluble tissue factor is released from endothelial cells in response to inflammatory cytokines. *Circ Res* 2005; 96:1233–1239

43. Brandtzaeg P, Sandset PM, Joø GB, et al: The quantitative association of plasma endotoxin, antithrombin, protein C, extrinsic pathway inhibitor and fibrinopeptide A in systemic meningococcal disease. *Thromb Res* 1989; 55:459–470

44. Akira S, Takeda K: Toll-like receptor signalling. *Nat Rev Immunol* 2004; 4:499–511

45. Kim JS, Park DW, Lee HK, et al: Early growth response-1 is involved in foam cell formation and is upregulated by the TLR9-MyD88-ERK1/2 pathway. *Biochem Biophys Res Commun* 2009; 390:196–200

46. Takaoka A, Wang Z, Choi MK, et al: DAI (DLM-1/ZBP1) is a cytosolic DNA sensor and an activator of innate immune response. *Nature* 2007; 448:501–505

47. Hornung V, Latz E: Intracellular DNA recognition. *Nat Rev Immunol* 2010; 10:123–130

48. Ye X, Ding J, Zhou X, et al: Divergent roles of endothelial NF-kappaB in multiple organ injury and bacterial clearance in mouse models of sepsis. *J Exp Med* 2008; 205:1303–1315

49. Song D, Ye X, Xu H, et al: Activation of endothelial intrinsic NF-{kappa}B pathway impairs protein C anticoagulation mechanism and promotes coagulation in endotoxemic mice. *Blood* 2009; 114:2521–2529

50. Chantrathammachart P, Mackman N, Sparkenbaugh E, et al: Tissue factor promotes activation of coagulation and inflammation in a mouse model of sickle cell disease. *Blood* 2012; 120:636–646

51. Knuefermann P, Baumgarten G, Koch A, et al: CpG oligonucleotide activates Toll-like receptor 9 and causes lung inflammation in vivo. *Respir Res* 2007; 8:72

52. Itagaki K, Adibnia Y, Sun S, et al: Bacterial DNA induces pulmonary damage via TLR-9 through cross-talk with neutrophils. *Shock* 2011; 36:548–552

53. József L, Khreiss T, Filep JG: CpG motifs in bacterial DNA delay apoptosis of neutrophil granulocytes. *FASEB J* 2004; 18:1776–1778

54. Henke PK, Mitsuya M, Luke CE, et al: Toll-like receptor 9 signaling is critical for early experimental deep vein thrombosis resolution. *Arterioscler Thromb Vasc Biol* 2011; 31:43–49